STYRELSEN FÖR

VINTERSJÖFARTSFORSKNING

WINTER NAVIGATION RESEARCH BOARD

Research Report No 87

Aki Kinnunen, Maria Tikanmäki, Jaakko Heinonen, Juha Kurkela, Pekka Koskinen and Matti Jussila.

AZIMUTHING THRUSTER ICE LOAD CALCULATION

Finnish Transport Safety Agency

Finnish Transport Agency

Finland

Swedish Maritime Administration

Swedish Transport Agency

Sweden

Talvimerenkulun tutkimusraportit – Winter Navigation Research Reports
ISSN 2342-4303
ISBN 978-952-311-036-6

FOREWORD

In its report no 87, the Winter Navigation Research Board presents the outcome of the project on azimuthing thruster ice load calculation development.

The approach for the development of the ice class rules is to determine ice load scenarios and load cases to be included in the ice class rules. The ice loads will be calculated with sophisticated models and the models will be verified with measurement data. Simplified load formulae will be developed based on ice load models and measurement data. The results will be combined to form the technical draft of Finnish-Swedish Ice Class Rules for azimuthing propulsion units. In this document, the work done during 2011–2012 is documented. The relevant load scenarios and applicable ice load calculation methods are presented, example cases selected and ice loads calculated for these example cases with different methods.

The Winter Navigation Research Board warmly thanks Mr. Aki Kinnunen, Ms. Maria Tikanmäki, Mr. Jaakko Heinonen, Mr. Juha Kurkela, Mr. Pekka Koskinen and Mr. Matti Jussila for this report.

Helsinki and Norrköping

June 2014

Jorma Kämäräinen

Finnish Transport Safety Agency

Peter Fyrby

Swedish Maritime Administration

Tiina Tuurnala

Finnish Transport Agency

Stefan Eriksson

Swedish Transport Agency

RESEARCH REPORT

VTT-R-08842-12

Azimuthing thruster ice load calculation

Authors: Aki Kinnunen, Maria Tikanmäki, Jaakko Heinonen, Juha Kurkela, Pekka Koskinen, Matti Jussila

Confidentiality: Public

Report's title	
Comparison of ice load models for azimuthing thruster ice load calculation	
Customer, contact person, address Finnish Transport Safety Agency Jorma Kämäräinen PO Box 320, FI-00101 Helsinki, Finland	Order reference
Project name AZIRULE2012	Project number/Short name
Author(s) Aki Kinnunen, Maria Tikanmäki, Jaakko Heinonen, Juha Kurkela, Pekka Koskinen, Matti Jussila	Pages 40/
Keywords Ice load, dynamic model, ice structure interaction, ice class rules	Report identification code VTT-R-08842-12

Summary

The approach for the development of the ice class rules is to determine ice load scenarios and load cases to be included in the ice class rules. The ice loads will be calculated with sophisticated models and models will be verified with measurement data. Simplified load formulae will be developed based on ice load models and measurement data. The results will be combined to form the technical draft of Finnish-Swedish Ice Class Rules for azimuthing propulsion units.

In this document, the work done during 2011 - 2012 is documented. The relevant load scenarios and applicable ice load calculation methods are presented, example cases selected and ice loads calculated for these example cases with different methods.

It can be concluded that the impact load model give loads that are at a correct range but validation regarding the dynamic system excitation is still needed before the simplified load models can be formulated. The ridge penetration model development show a good correlation with the full scale measurements and next step will be development of the simplified load model for ice class rules. It has become evident that load models for the dynamic excitation for dynamic analysis are needed for the ice class rules. The proposal is to derive the load excitation based on the propeller ice load models that have been used for the development of the present Finnish Swedish Ice Class Rules for Propulsion Machinery.

Confidentiality	Confidential

Espoo 17.2.2013

Written by	Reviewed by	Accepted by
Aki Kinnunen Research Scientist	Matti Jussila Senior Scientist	Johannes Hyrynen Technology Manager

VTT's contact address

Distribution (customer and VTT)
Trafi, Jorma Kämäräinen, PDF and 3 paper copies
VTT, 1 copy

Contents

1 Introduction

The Finnish Transport Safety Agency (Trafi) initiated ice class rule development project for azimuthig thrusters. Finnish-Swedish ice class rules do not have at the moment specific (ice class) rules for azimuthing thrusters.

Into the project steering group were invited representatives from classification societies and azimuthing thruster manufacturing industry in order to get the ice class rule development work onto right track right from the start. VTT Technical Reasearch Centre of Finlad is responsible of the actual development work, following the guideline frames set by the steering group.

A project kick-off meeting was held in June 2010 in Helsinki, with a very good attendance from the invited classification societies and industry partners. The initiative meeting was followed by participator survey regarding what to study in this project.

The work progress was followed up in steering group meetings, held annually in 2011 and 2012.

In this document the 2011 - 2012 activities and key results are presented.

Simplified load formula for ice class rules are to be developed further in the following years project(s).

2 Goal

The ice class rule development is aimed to be harmonized with international ice class rule work. The approach is to determine ice load scenarios and load cases to be included in the ice class rules. The ice loads will be calculated with sophisticated models and models will be verified with measurement data. Simplified load formulae will be developed based on ice load models and measurement data. The results will be combined to form the technical draft of Finnish-Swedish Ice Class Rules for azimuthing propulsion units.

For 2011 - 2012, goal was to

Implement ship and thruster geometry for ridge penetration FEM modelling and run a parametric study, including variation of ship size, thruster size, thruster angle and ridge geometry
- Review available full scale data for validation purposes; measurements from ice breaker Fennica and Botnica were available, Fennica results were considered first for validation
- Create FEM model of Fennica, and run ridge penetration simulations
- Ice block impact model was to be further developed, to describe structural damping, improve ice-structure contact force model functionality.

3 Ice load scenarios

The relevant ice load scenarios for ice structure interaction are shortly described here. Further details for ice load calculation for each scenario are documented in the ice load model and calculation chapters.

3.1 Ice impact

The main parameters when an individual ice block impact to the propulsion structure are the affecting ice mass *m* (kg) and initial relative velocity *v* (knots) between the ice and structure. Relevant scenarios include at least impact to propeller hub and 'rear end of propulsion unit'. The relevant load calculation models include at least: VTT, ABS and DNV ice load models. Following figure illustrates the load scenario.

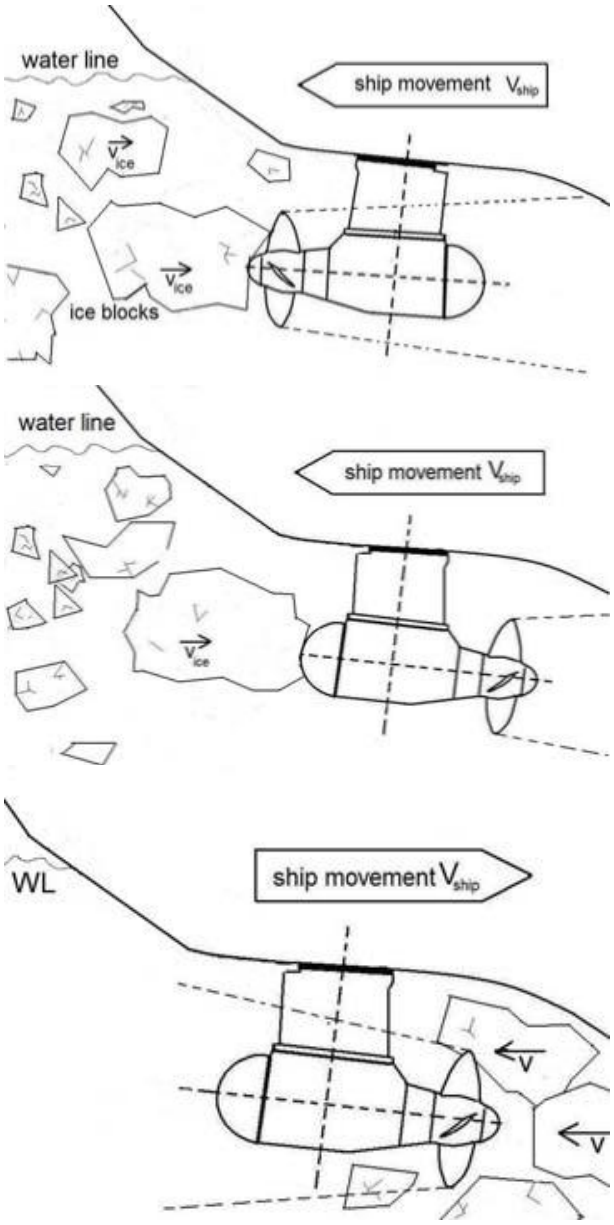

Figure 1. Ice impact load scenario.

3.2 Ridge penetration

Ice ridges are common ice features in Northern seas. They are formed when sea ice is compressed or sheared under the action of wind and currents. A ridge contains a large number of ice pieces of varying sizes and shapes that are piled arbitrarily. Rubble above the water line is called a sail and the rubble below the water line is called a keel. Between them, close to the waterline, is the re-frozen solid ice zone called a consolidated layer, Figure 2. First-year ridges are often a key consideration from an engineering perspective.

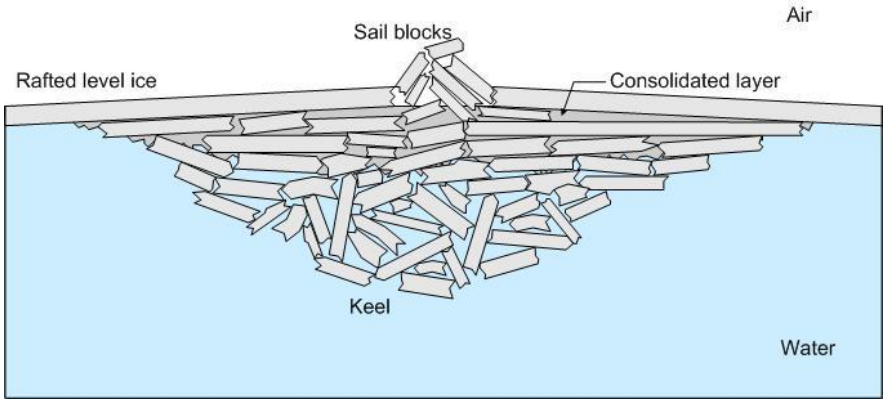

Figure 2. Principal sketch of ice ridge.

The relevant load calculation methods include finite element simulations (FEM) and corresponding ice load predictions according to DNV. Even though the FEM simulation with advanced ice failure model requires very intensive computation and is fairly complicated to use, it gives basic understanding of failure mechanisms of ice and of ice load development during ice-thruster interaction. This approach can then be further utilized for instance to develop a simplified ice pressure distribution model.

The worst scenario to introduce the highest loads on the thruster body was assumed, when the thruster was turned sideways before interacting with an ice ridge (see Fig. 3). The other steering angles can be straightforwardly studied by the FEM-analysis.

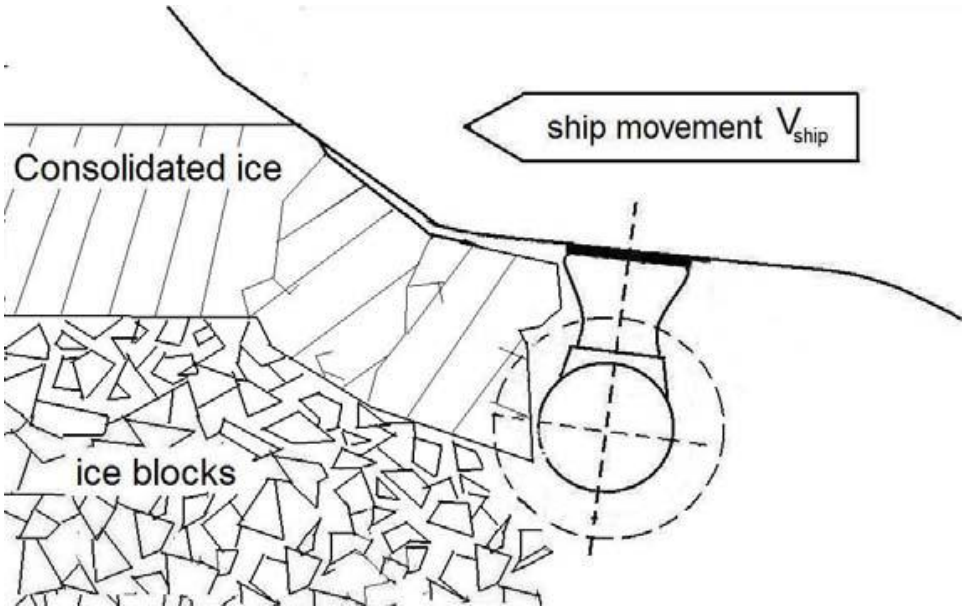

Figure 3. Ridge penetration load scenario.

4 Limitations

4.1 Load scenarios not included

Propeller milling ice, propeller contacting to ice directly or radially and propeller blade bending considerations are not yet included in this study.

5 Included ice load models

Description of included ice load models theoretical background follows.

5.1 Impact model with structure dynamics, VTT impact model

5.1.1 General

In VTT impact model forces between ice block and the propeller hub are calculated as a function of time during the impact. The propeller penetrates to the ice block during the impact. The reaction force affecting in the connection of the ship and the thruster is calculated from the contact force. Maximum values of the contact force and the reaction force are used to estimate the realistic loads for the ships service life. Figure 4 illustrates the impact between the thruster and the ice block.

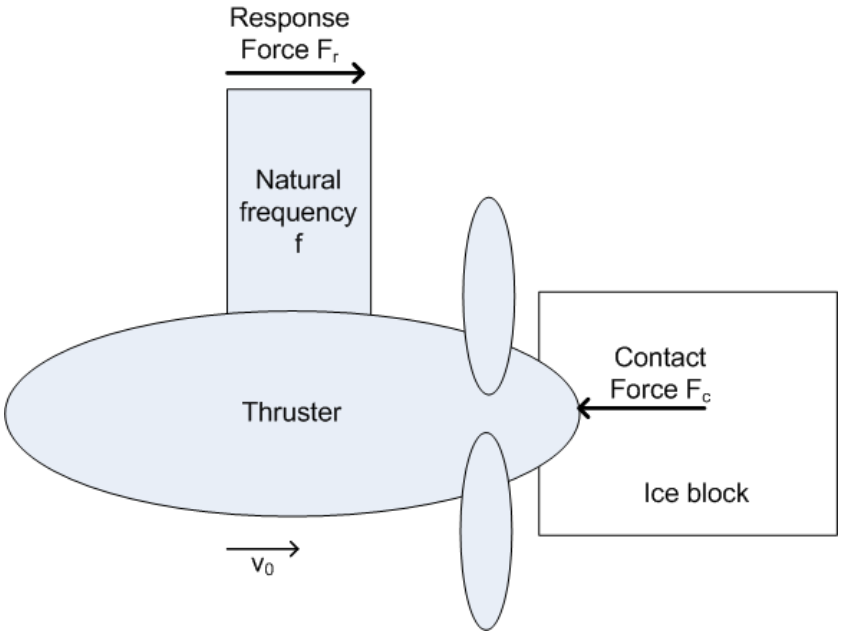

Figure 4. Sketch of the impact between the thruster and the ice block as estimated in VTT impact model.

5.1.2 Indentation pressure

The contact area grows when penetration goes further. This means that the contact force grows because indentation pressure p is a function of contact area A and it is defined by

$$p = p_0 \sqrt{\frac{A_0}{A}} \quad (1)$$

where A_0 is a reference area and p_0 is a reference pressure which are in this case 1 m^2 and 3 MPa respectively. Design curve for the indentation pressure and some full scale data points are shown in the Figure 5. Some full scale data points are from m/s Aatos (Huovinen, 1990) and rest of the data is collected from different sources by Bjerkås (2007)

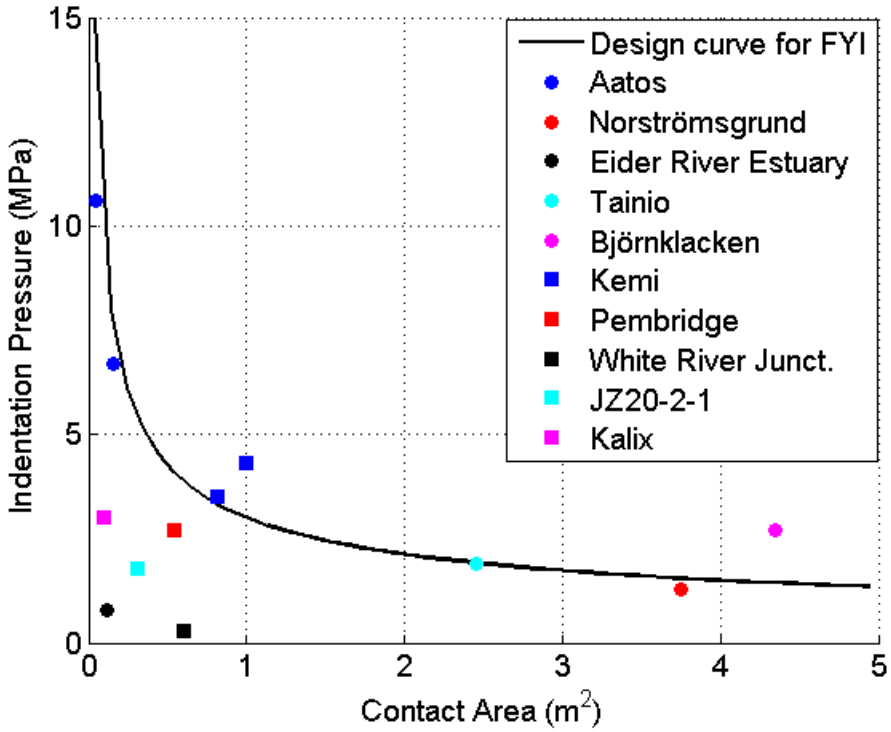

Figure 5. Indentation pressure as a function of contact area.

5.1.3 Description of the model – undamped case

During the impact contact force F_c and response force F_r are defined by equations

$$\begin{aligned} F_c - F_r &= m_t \ddot{u}_1 \\ -F_c &= m_i \ddot{u}_2 \end{aligned} \quad (2)$$

where m_t is mass of the thruster, m_i is mass of the impacting ice block and u_1 and u_2 are displacements as shown in Figure 6. Contact force F_c is based on indentation pressure and is determined by equation

$$F_c = p_0 \sqrt{A_0 A}, \quad (3)$$

where A is the current contact area defined by

$$A = \pi(r^2 - (r - u_2 + u_1)^2), \quad (4)$$

where r is radius of curvature of the thruster hub. Response force F_r is determined by equation

$$F_r = k u_1 \quad (5)$$

where $k$is the stiffness of the thruster which is calculated from the thruster's natural frequency f by

$$k = 4\pi^2 f^2 m_t. \quad (6)$$

Finally these equations are solved by difference methods with initial values

$$\begin{aligned} u_1(0) &= 0 \\ u_2(0) &= -t_0 v_0 \\ u_1(t_0) &= 0 \\ u_2(t_0) &= 0 \end{aligned} \quad (7)$$

where t_0 is the increment of time and v_0 is the speed of the vessel. Penetration ends when all the kinetic energy is used for ice crushing. Time history of the contact and response forces calculated from these equations by difference methods is shown in Figure 7. Places of the contact and the response force are shown in Figure 8. Figure 9 presents the effect of the mass of the ice block to the contact and response forces.

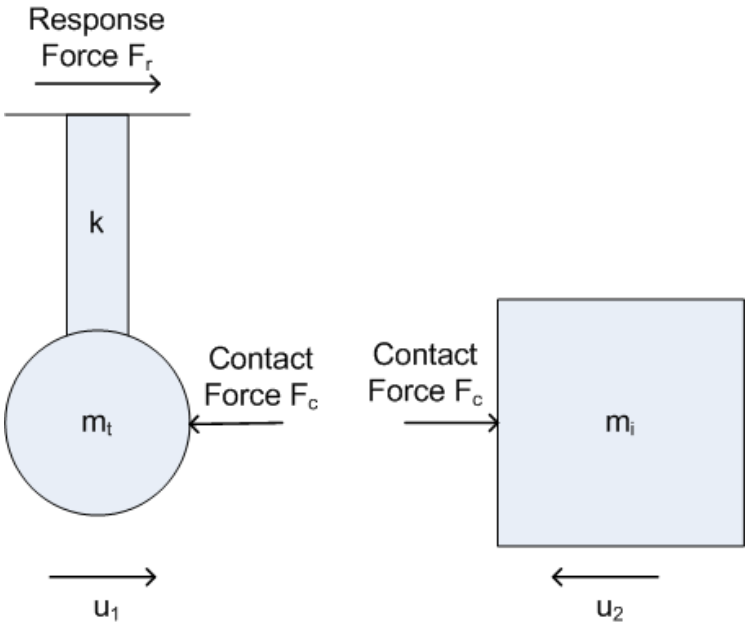

Figure 6. Symbols as they are used in VTT impact model.

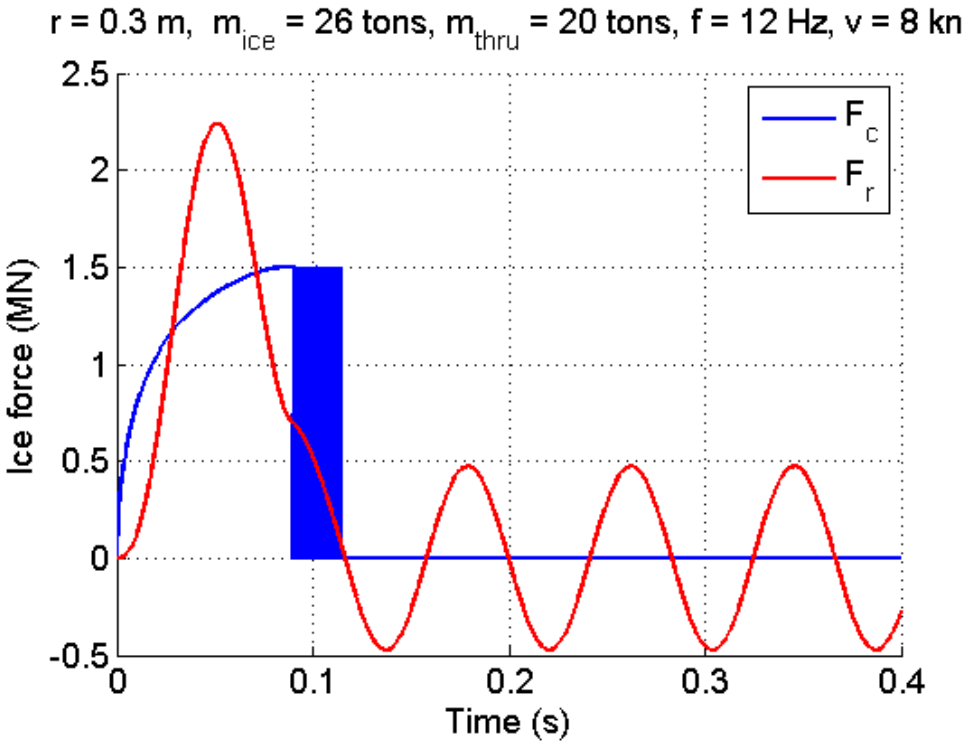

Figure 7. Time history of the contact and response forces when ice block is impacting to the thruster, where radius of the curvature of the thruster is 0.3 m, mass of the ice block is 26 tons, mass of the thruster is 20 tons, natural frequency of the thruster is 12 Hz and the vessel speed is 8 knots. The blue line corresponds to the contact force and the red line to the response force.

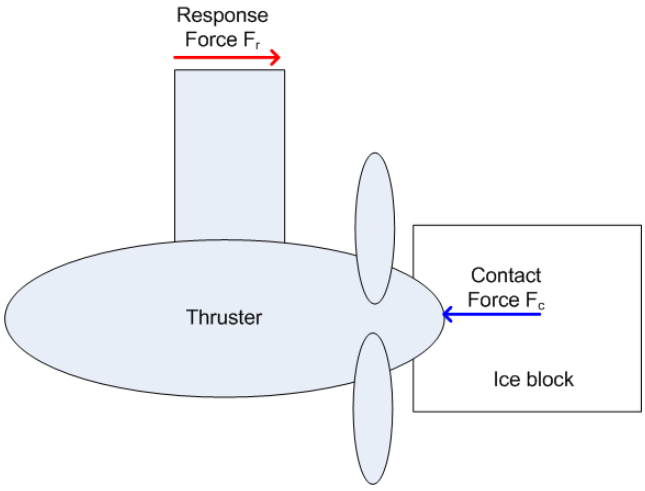

Figure 8. Places of the contact and the response force.

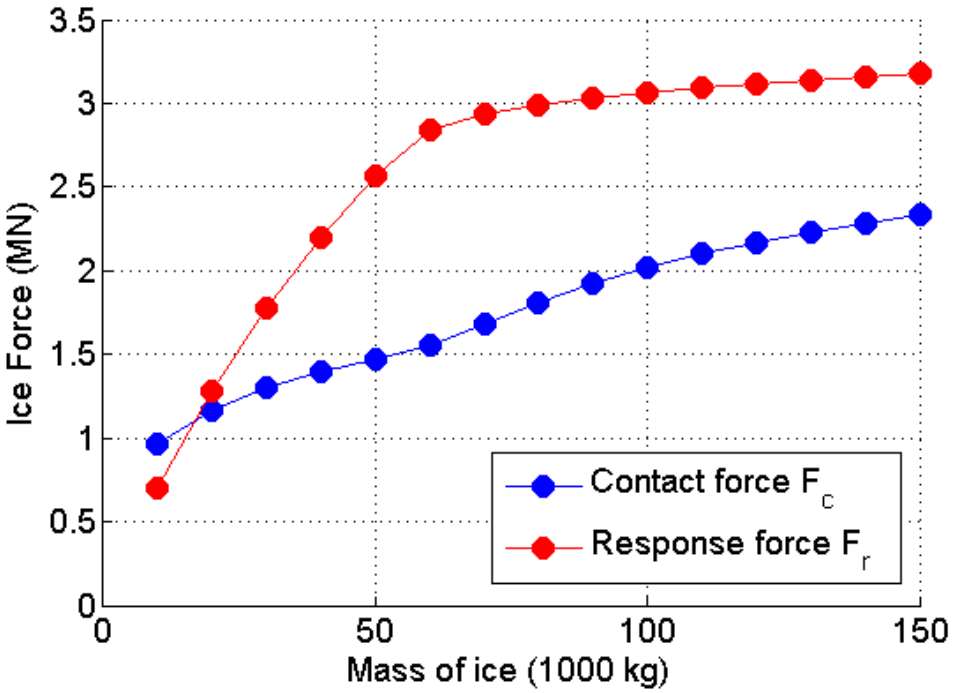

Figure 9. The effect of the mass of the ice block to the contact and response forces.

5.1.4 Structural damping in the model

The structural damping within the thruster structure is described as viscous damping, the damping force is relative to velocity.

5.1.5 Hydrodynamic contact force between ice and thruster

By assuming existence of water between the ice and thruster surface, the contact becomes like a hydrodynamic bearing. The sketch of Contact principle is shown in Figure 10. There is some distance between the ice and thruster surface, with water in between, having a known viscosity. The surfaces approach or move away from each other at some speed. These assumptions are used to apply hydrodynamic load calculation for the contact.

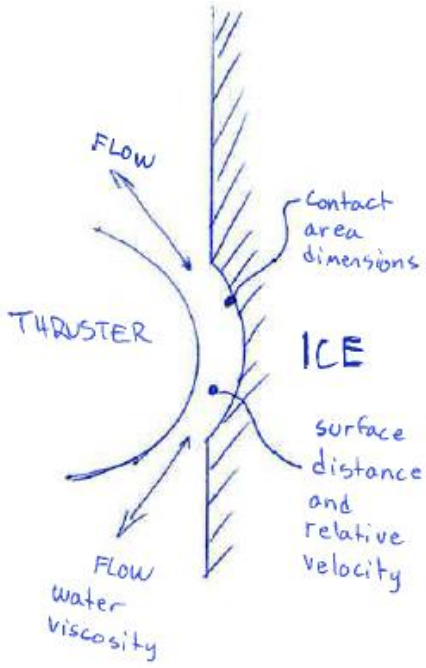

Figure 10. Contact principle for ice and structure submerged in water

The contact can be estimated with a circular plate and "infinite plate", as presented in CRC Handbook of lubrication, Figure 11:

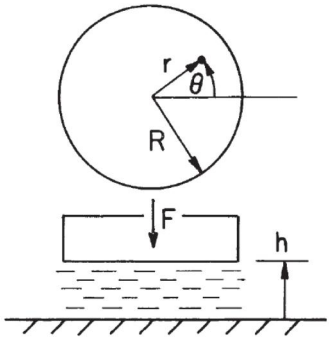

Figure 11. Theoretical approach for hydrodynamic force. CRC handbook of lubrication.

The force formulation is given with fluid layer thickness *h*, surface relative perpendicular velocity *hdot* , circular plate radius *R*, viscosity μ

$$F = \frac{-3\pi R^4}{2}\frac{\mu \dot{h}}{h^3} \qquad (8)$$

The model is suitable for describing compressive forces as well as tensile forces. On compression, the force is limited by the ice maximum strength as indicated by the contact pressure model. For tensile force, i.e. suction, the force is limited by the hydrostatic pressure at the depth of contact, meaning cavitation can occur in the contact and it limits the force to some level.

5.1.6 Linear elastic material model for ice

One drawback of the initial model was that it showed some numerical noise at contact opening, meaning contact force seemed to alternate between zero and maximum ice material allowed load for a relatively long period of time when the ice-structure contact started to separate.

This lead to thinking that material properties may have an effect on the simulation and assumption of linear elastic material model for ice was adopted into the model.

For the used difference method, the formulation of linear elastic model applied is

$$\begin{aligned} \varepsilon &= \frac{u_{max}-u_i}{L}, \\ \sigma &= E\varepsilon \end{aligned} \qquad (9)$$

Contact load solution is of type

$$F = F_{max} - A_i E \varepsilon \qquad (10)$$

where the strain ε is calculated from maximum thruster penetration into ice u_{max}, penetration at current time step u_i and scaled with the smallest ice block dimension L.This gives some softness to material behaviour and remarkably improves the numerical stability with this solution method. For practical application, the load release from full contact load to zero was achieved at 2-5 mm displacement.

5.1.7 Water flow induced drag force affecting ice block

Drag force induced from water flow affecting the ice block is approximated by ice block dimensions and drag force formula. The ice block orientation is fixed during calculation, and the block is assumed to have drag properties like a cube.

The drag force formula used is

$$F = \frac{1}{2} A \rho \, cd \, v^2 \qquad (11)$$

where A is the ice block area perpendicular to the flow, $\rho$is the water density, cd is drag coefficient, 1.05 in this case, and v is the effective flow velocity (or ice block velocity in fluid) at the ice block location.

5.1.8 Description of the model – damping, contact, linear-elastic, drag

Effect of the model parameters is shown in Figure 12.

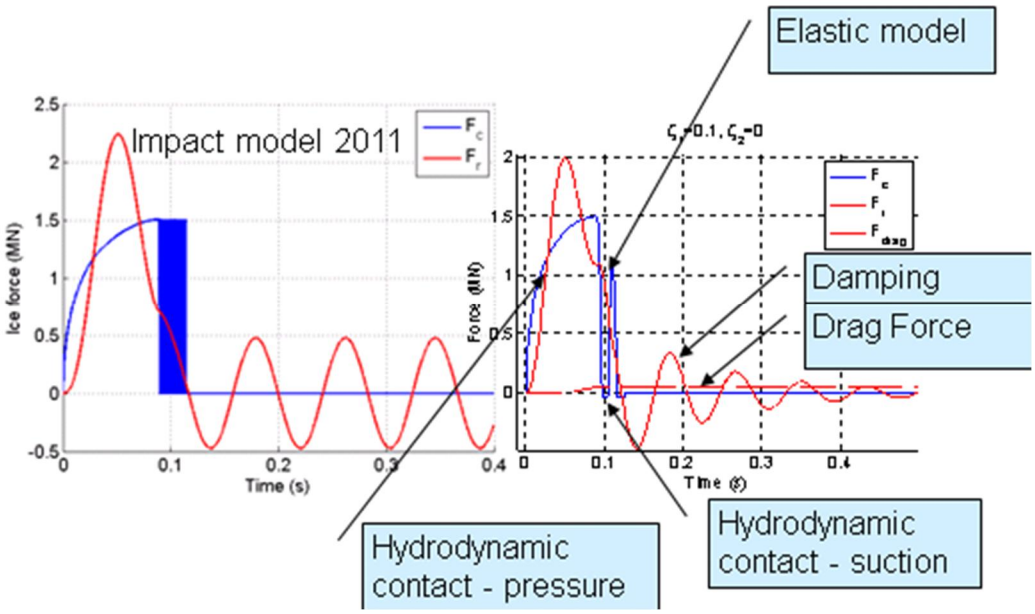

Figure 12. Example of simulated impact time history with non-damped model and model(left) with updated features (right)

The equation of motions used need to include the damping and are formulated as follows

$$\dot{u}_2(i) = \frac{u_2(i) - u_2(i-1)}{dt} \quad (12)$$

$$\dot{u}_1(i) = \frac{u_1(i) - u_1(i-1)}{dt} \quad (13)$$

$$F_{drag}(i) = \frac{1}{2} c d A_{ice}(i) \rho (v_0 - \dot{u}_2(i))^2 \quad (14)$$

$$F_r(i) = k u_1(i) + c_1 \dot{u}_1(i) \quad (15)$$

$$u_2(i+1) = \frac{-F_c(i) + F_{drag}(i) + c_2(\dot{u}_2(i) - \dot{u}_1(i))dt^2}{m_{ice}} + 2u_2(i) - u_2(i-1) \quad (16)$$

$$u_1(i+1) = \frac{F_c(i) - F_r(i) - c_2(\dot{u}_2(i) - \dot{u}_1(i))dt^2}{m_{thru}} + 2u_1(i) - u_1(i-1) \quad (17)$$

Response force is *Fr*, flow-induced drag force *Fdrag*, contact load *Fc* is described by the hydrodynamic contact load, limited on compression to ice strength and on tension, to hydrostatic pressure.

5.1.9 Limitations of the model

At the moment impact model does not take influence of thruster induced forces (thrust, flow field) into account. Only hemispherical indentator has been implemented so far. Influence of e.g. thrust and other indentator shapes may be implemented to the model in the future.

5.2 FEM simulation of ridge penetration

5.2.1 General

FEM simulation results in valuable information of thruster-ice interaction, which is difficult to gain by other methods. One can observe from simulations which failure mode of ice takes place during thruster interaction or what is the influence of ridge composition, ice thickness etc. Simulation results can be utilized to develop simplified equations for ice load predictions. However, the validation with full-scale data is required.

5.2.2 Material models to describe ice failure

The material models for ice ridge and FEM-model development for the ice-thruster interaction were carried out in a previous AHRAVUO-project (http://ahravuo.vtt.fi/, Heinonen, 2004). These include a material model for the ice rubble and a model for the consolidated layer which describe the failure of ice. These models have been implemented into Abaqus finite element software. Figure 13 illustrates a shear-cap failure criterion for ice rubble in stress space. The material parameters were evaluated according to full-scale measurements in Gulf of Bothnia. In these tests, the mechanical properties of ice ridge were measured by different type of loading tests during five winters (Heinonen, 2004).

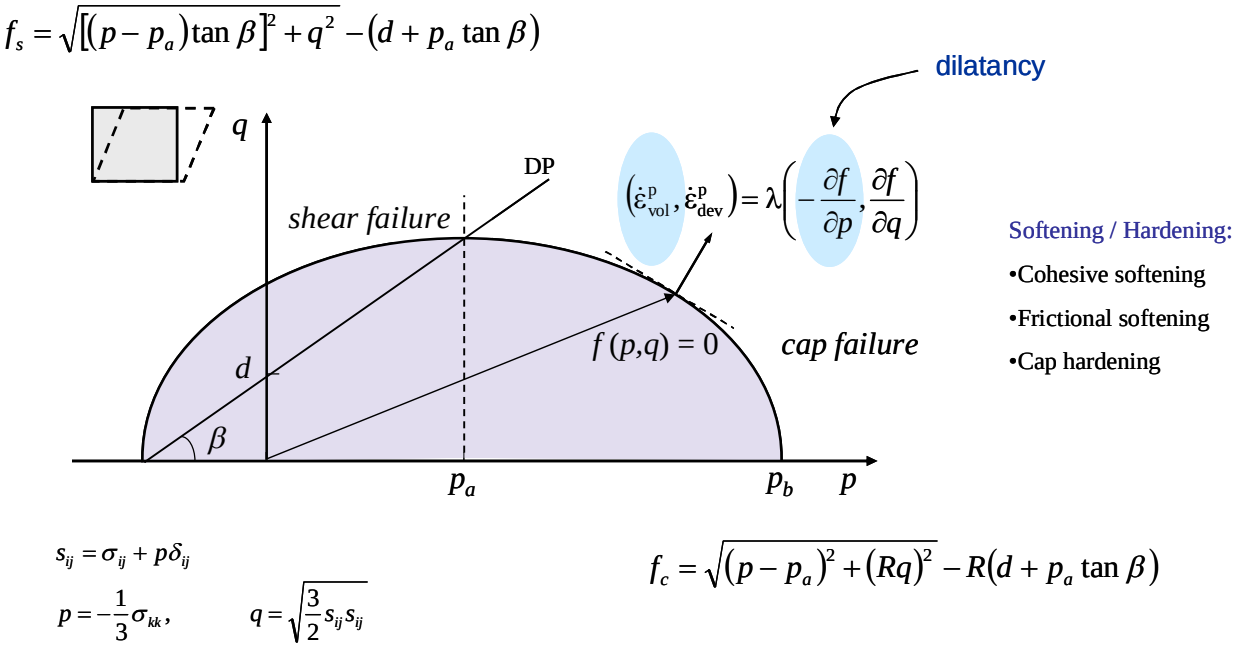

Figure 13. Shear-cap failure criterion in stress space for ice rubble introducing the shear failure and the compaction failure (Heinonen, 2004).

5.2.3 Finite element model

The FEM model for ice-thruster interaction is shown in Figure 14. The ridge is modeled by deformable elements including the failure criterions as mentioned above. The ship body and the thruster are modeled by rigid elements, because the stiffness of these parts is high compared to ice. Therefore, the deformations of thruster or ship body do not influence on the ice loads significantly.

The ridge was modeled to float on the water by controlling the vertical position with the gravitation and buoyancy forces. The ridge was idealized to include three layers of constant thicknesses: the sail, the consolidated layer and the keel. The ridge field was assumed half-infinite in the horizontal direction by utilizing infinite elements at the circular edge (see e.g. Figure 22). The ship body with the thruster was moved horizontally towards the free edge of the ridge. The steering angle was varied.

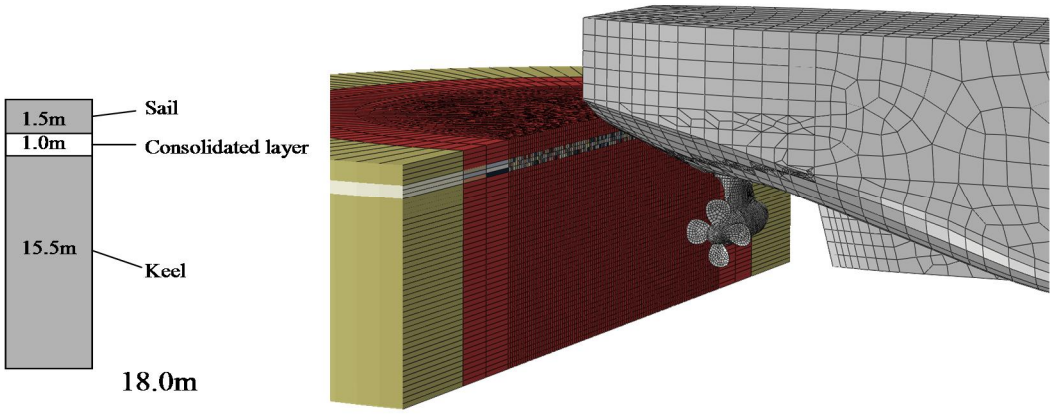

Figure 14. FEM model for ice-thruster interaction. At left: main dimensions of selected ridge. At right: the idealized ridge is floating on the water and the ship body with a thruster is moving horizontally towards the ridge. The steering angle is 90 degrees. The model represents a large scale thruster.

6 Results

Load calculation examples and result comparison for selected load scenarios and load models follow in this chapter.

6.1 Ice impact model application: case Fennica

The Fennica case VTT impact model calculations (Chapter 5.1) are based on assumption that ice block will hit to the “head” of thruster, see Figure 15.

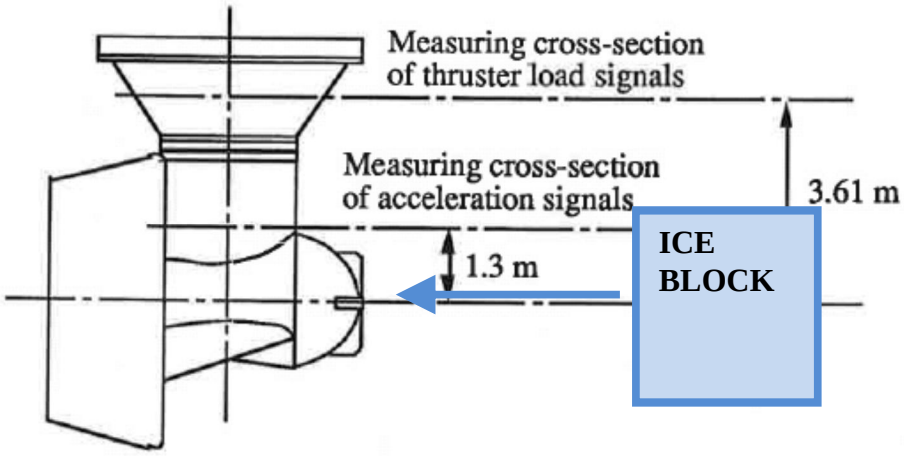

Figure 15. Ice block impact principle for Fennica

Thruster parameters used for calculation are

- Effective dynamic mass of the thruster 50 tons
- Thruster head radius 1.20 meters
- Speed at contact time 6 and 12 knots
- Depth of contact 4 meters
- Natural frequency known

Ice parameters used for calculation are

- Ice block masses according to classes IC .. IA Super, 6 tn … 32tn
- Uniaxial ice compression strength 3 MPa

This gives some parameter space, resulting a set of results. Examples of simulated time histories are in following figure (ice class IA Super, left 12 knots, right 6 knots).

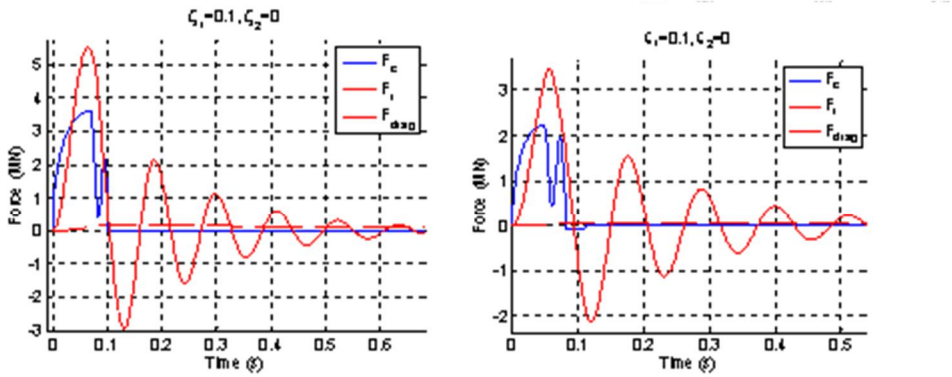

Figure 16. Calculated impact load time history for Fennica thruster, ice block for class IA Super, *speed 12 knots (left) and 6 knots (right).*

The maximum contact force Fc and maximum response force Fr for calculated cases are in Table 1.

Table 1. Maximum contact forces and response forces for classes IC … IA Super *and speeds 6 and 12 knots.*

Ice Class	Hice [m]	m_ice [t]	Fmax [MN], 6kn Fc	Fr	Fmax [MN], 12kn Fc	Fr
IC	1	6,0	1,38	0,92	2,17	1,78
IB	1,2	10,4	1,62	1,47	2,55	2,82
IA	1,5	20,3	1,96	2,52	3,11	4,68
IA Super	1,75	32,2	2,24	3,48	3,61	5,50

6.1.1 Simplified load formula for impact

One target in the project is to develop load formula for impact, and a suggestion of load formula type is calculation of ice contact load and estimating structure response with a some dynamic magnification factor.

Contact load can be of type

$$F_c = f(\sigma_{ice}, m_{ice}, v, shape, scale) \quad (18)$$

Here, the ice class rule based parameters can be *ice strength*, *ice mass*, *impact velocity* and thruster related parameters can be *shape* and *scale*, describing the shape of impacting (thruster)structure and some scaling factor, showing how big the impacting (thruster)structure is.

For response force, the contact force is multiplied by dynamic magnification factor, like

$$F_r = C_0 F_c \quad (19)$$

Of course, careful work is needed to evaluate if this approach is feasible and is it possible to establish reasonable response force estimate with this approach.

Impact load model validation with controlled experiment as well as with full scale data is crucial to maintain strong arguable physical basis for the load models.

As the impact model may be capable of estimating the single event load, the question of how many impacts (and what magnitude) does thruster encounter in regular use for a given time period, needs discussion of its own. A sort of “impact occurrence histogram or profile” or some other statistical approach might be useful.

6.2 Ridge penetration

6.2.1 Ridge penetration principles

Simulations resulted in pressure distributions on the thruster body. Figure 17 introduces the cross section view along the symmetry axis of ridge. Therefore, only part of the thruster and ship body is shown. One observes that ship hull push the consolidated layer downwards causing increased pressure in the front of the body. Although the ship hull fails the consolidated layer by bending it downwards, increased pressure makes the underlying rubble stronger. That has a disadvantage to increase the loads on thruster body due to ice rubble.

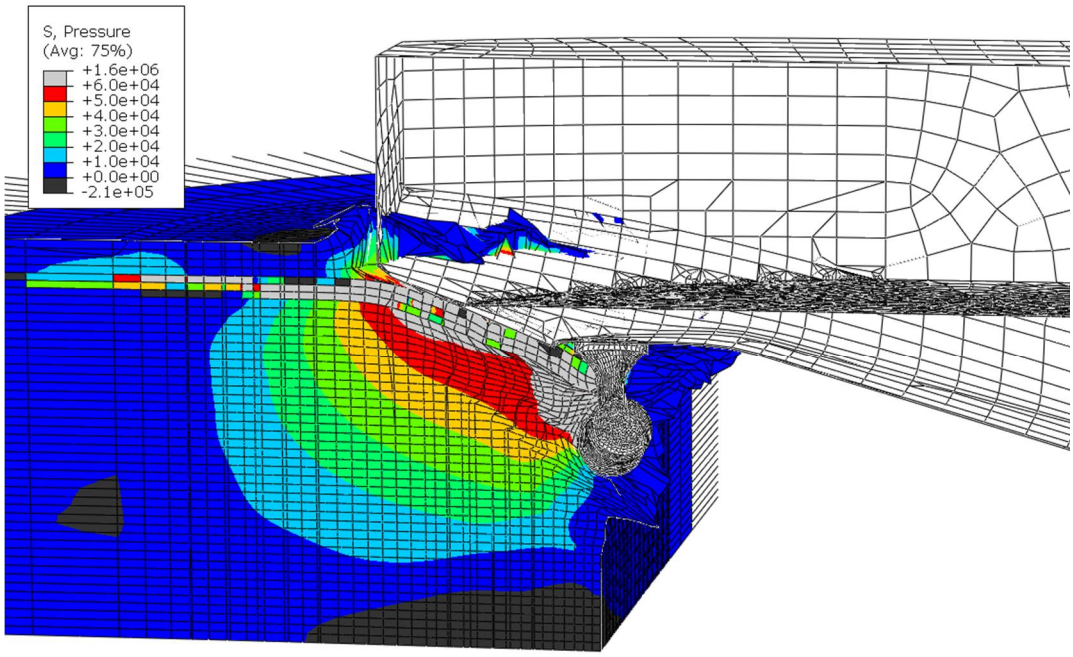

Figure 17. Pressure stress distribution in ridge during thruster penetration. Cross section view along the symmetry axis of ridge. Therefore, only part of the thruster and ship body is shown. The light grey area represents pressure over 60kPa and dark grey area below zero.

Figure 18 represents the ice pressure distribution on the thruster and ship hull at one selected time instant. Due to non-simultaneous ice failure, high pressures occur only in few spots. The locations of spots vary continuously. These spots represent the load mostly due to the consolidated layer of the ridge, which is observed from Figure 17.

Ice pressure distribution depends much on the size of the thruster and the composition of ridge. The thicker the consolidated layer is, the larger the high pressure region is.

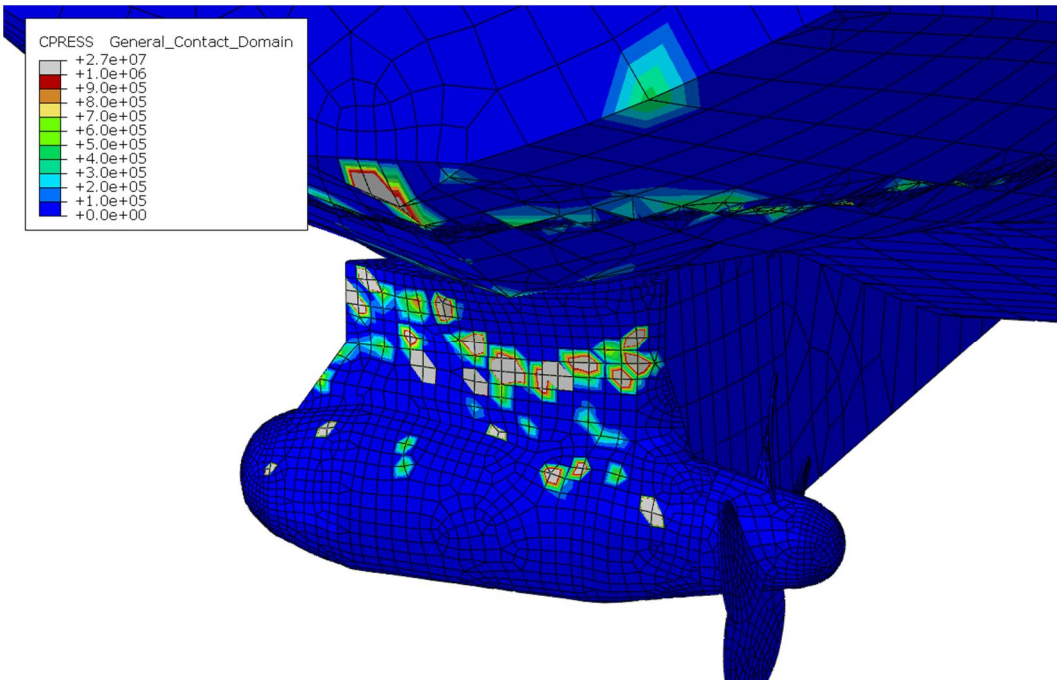

Figure 18. Ice pressure stress distribution on the thruster body during ridge penetration. Therefore, only part of the thruster is shown. The light grey area represents pressure over 1MPa.

6.2.2 Ridge penetration parametric studies

Set of model parameters were varied to gain basic understanding of effect of different parameters. The parameter sets used were

- Large and small thruster
- Typical and extreme ridge by varying the ridge thickness
- Ridge penetration speed variations

6.2.2.1 Ice ridge

Figure 19 shows the dimensions of two ridge types used in the simulations. The layers in a typical ridge are the sail 0.4 m, the consolidated layer 1.0 m and the rubble 4.0 m. The layers in an extreme ridge are the sail 0.8 m, the consolidated layer 1.75 m and the rubble 8.25 m.

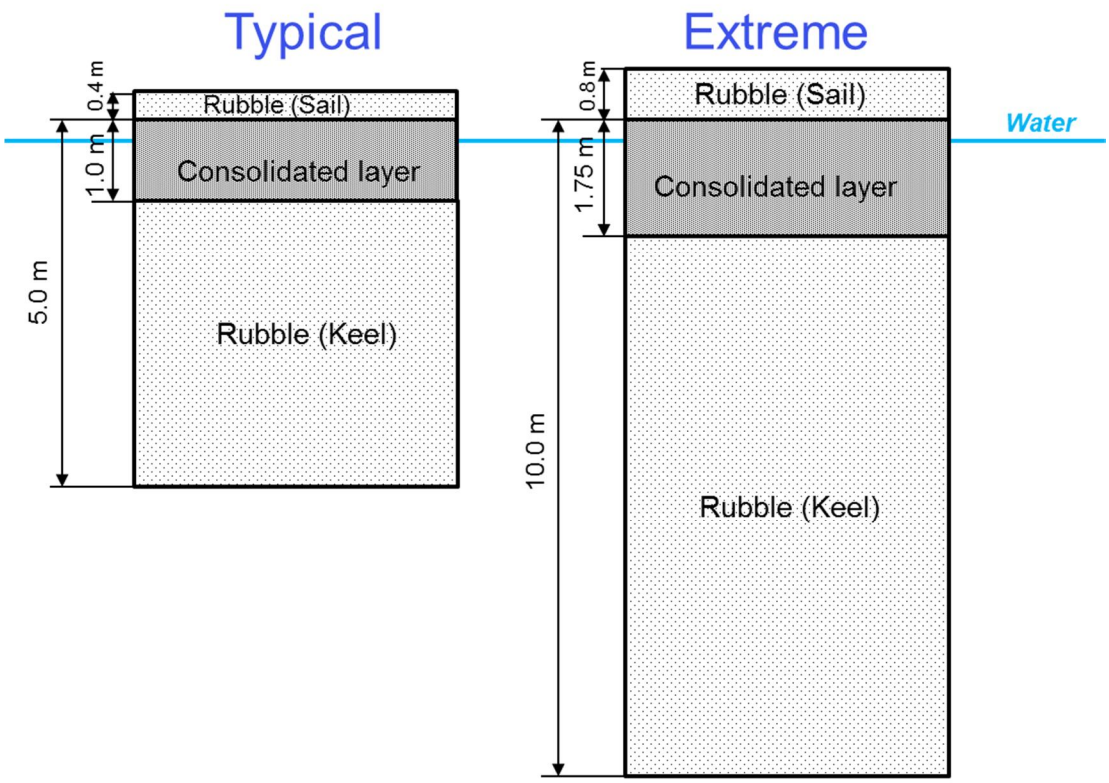

Figure 19. Ridge types for parameter runs.

6.2.2.2 Ice properties

The consolidated layer was divided into five (typical ridge) or nine (extreme ridge) layers in the thickness direction. Mechanical properties: elastic modulus, compressive and tensile strength were varied randomly such that each layer consisted of ten different material properties with the same mean and standard deviation as obtained in the material tests. Concrete Damaged Plasticity –model (CDP) was applied to simulate the failure of the consolidated layer. Mechnical properties of consolidated layer are listed in Table 2 and Table 3. Ice density was ρ = 900 kg/m^3. Tensile strength was about 8 % from compression strength.

Table 2. Consolidated layer ice properties, typical ridge.

Depth [m]	Temp. [°C]	E_{ave} [GPa]	E_{stdev} [GPa]	$S_{c,ave}$ [MPa]	$S_{c,stdev}$ [MPa]
0.1000	-2.0000	0.7047	0.3110	4.4022	1.6269
0.3000	-2.0000	0.9418	0.3300	6.2205	1.3964
0.5000	-2.0000	0.8441	0.2829	5.2417	0.9353
0.7000	-2.0000	0.5322	0.2035	3.3865	0.6634
0.9000	-2.0000	0.0881	0.0290	1.3790	0.4220

Table 3. Consolidated layer ice properties, extreme ridge.

Depth [m]	Temp. [°C]	E_{ave} [GPa]	E_{stdev} [GPa]	$S_{c,ave}$ [MPa]	$S_{c,stdev}$ [MPa]
0.0972	-2.0000	0.6992	0.3220	4.3500	1.6530
0.2917	-2.0000	0.7655	0.2948	4.8865	1.5297
0.4861	-2.0000	0.9125	0.3242	5.9982	1.4186
0.6806	-2.0000	0.9073	0.3088	5.8411	1.1805
0.8750	-2.0000	0.8441	0.2829	5.2417	0.9352
1.0694	-2.0000	0.7383	0.2711	4.4636	0.8241
1.2639	-2.0000	0.4546	0.1742	3.0196	0.6078
1.4583	-2.0000	0.0916	0.0360	1.3123	0.3553
1.6528	-2.0000	0.0857	0.0243	1.4234	0.4664

Cohesion value and friction angle of the ice rubble are d = 6000 N/m^2 and β = 35°. Density of ice rubble is ρ = 642 Kg/m^3, elastic modulus is E = 1.1e+08 N/m^2. Poisson's value ν = 0.3 and friction coefficient in ice-structure contact μ = 0.15.

6.2.2.3 Thrusters and hulls

Simulations were made for two different sizes of the truster, a large (cross-section area 42 m^2) and respectively a small (6 m^2). The model of the thruster is shown in Figure 20. The geometrical shape is same for both cases and the derired cross-sectional size is adjusted by scaling. The dimensions for the large thruster are: length 10.65 m, diameter 3.0 m and propeller diameter 5.6 m and for the small, respectively, 4.05 m, 1.11 m and 2.13 m.

A simplified geometry was applied to model ship hull, as shown in Figure 21. The length of the model of large hull is 64.8 m and the width 23.1 m. And for the small hull respectively, 24.6 m and 8.8 m.

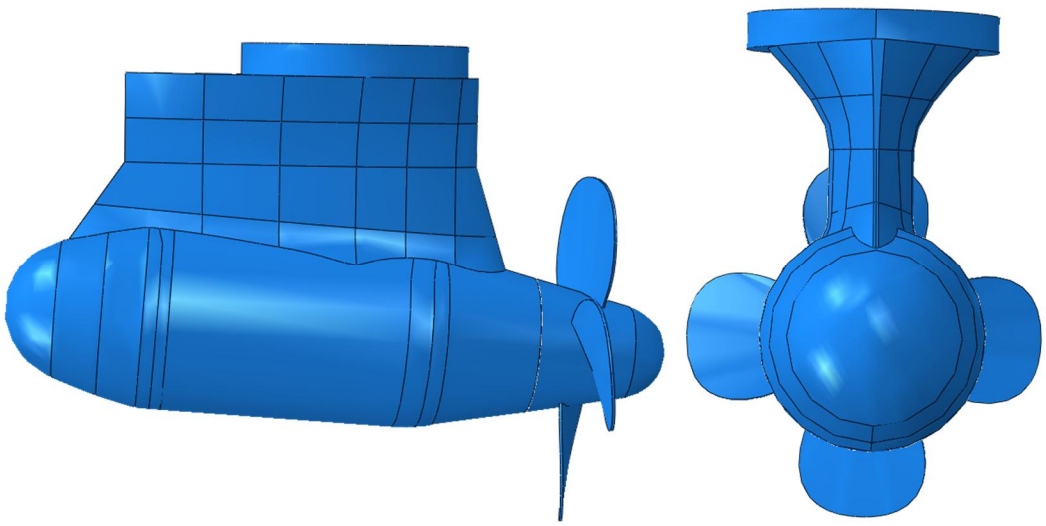

Figure 20. Model of the thruster.

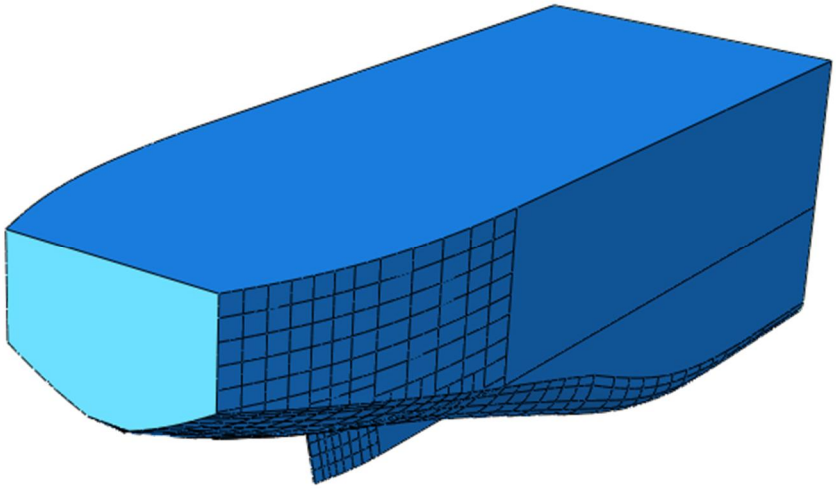

Figure 21. The geometric model of ship hull. Only the aft part of the hull was modelled.

6.2.2.4 FEM models and simulation

A parametric study was carried out by varying following quantities:

- ridge type is typical or extreme
- hull is small or large
- ship speed is 2 knot or 4 knot (constant)
- thruster angle is 0°, 45° or 90°.

Figures 22 - 25 introduce FEM-model for parameter study. Middle part of the model was discretized with dense element mesh and the far-end boundary region with sparse mesh. In the vertical direction the element size in sail was 100 – 200 mm, in the consolidated layer 200 mm and in the rubble 400 mm. In the lateral plane the element size was 400 – 500 mm. Model properties are listed in Table 4.

Numerical simulations were performed by Abaqus/explicit 6.12.1 program. Element types were C3D8R (ice), CIN3D8 (ice infinity), R3D3 and R3D4 (hull, thruster and propeller). The hull, thruster and propeller were assumed fully rigid. Simulation time was 7.5 – 50 s, corresponding 15.4 – 51.4 m movement of the ship.

Table 4. Fem model properties.

Model	Model size	Dense mesh	Infinity edge	Number of elements
Typical + small	50 x 100 m^2	22 m	18 m	83227
Typical + large	100 x 200 m^2	50 m	30 m	168767
Extreme + small	50 x 100 m^2	22 m	18 m	131227

Extreme + large	100 x 200 m^2	50 m	30 m	283967

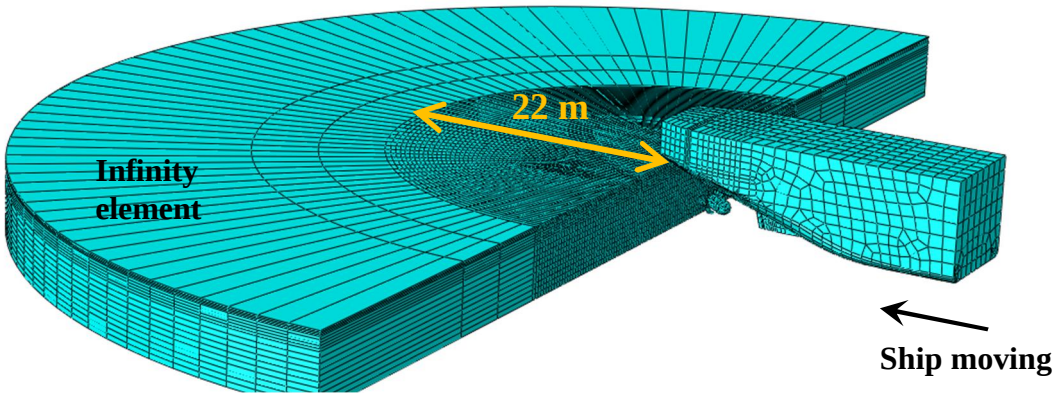

Figure 22. Typical ridge + small hull.

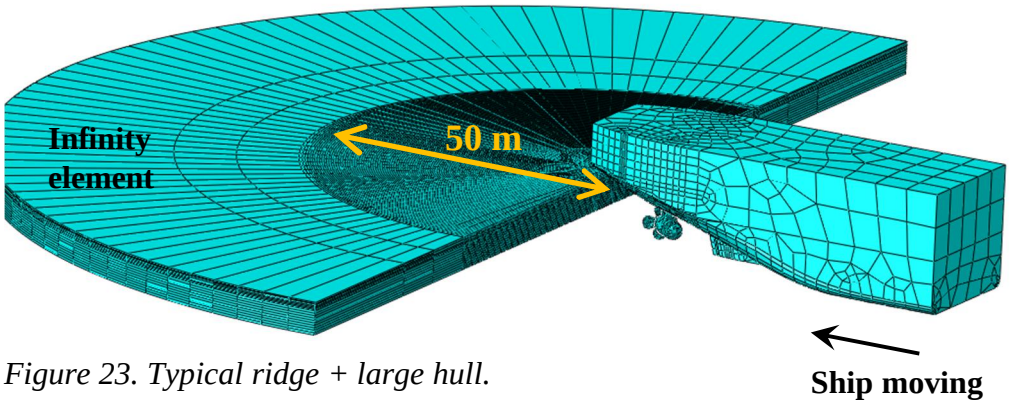

Figure 23. Typical ridge + large hull.

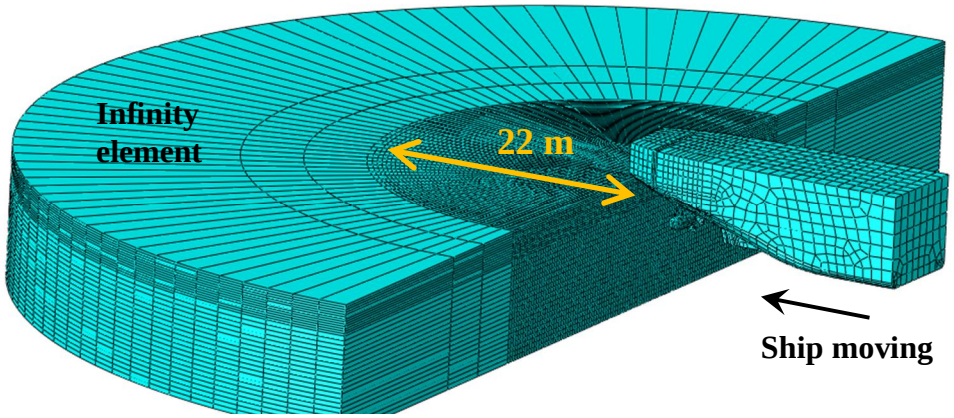

Figure 24. Extreme ridge + small hull.

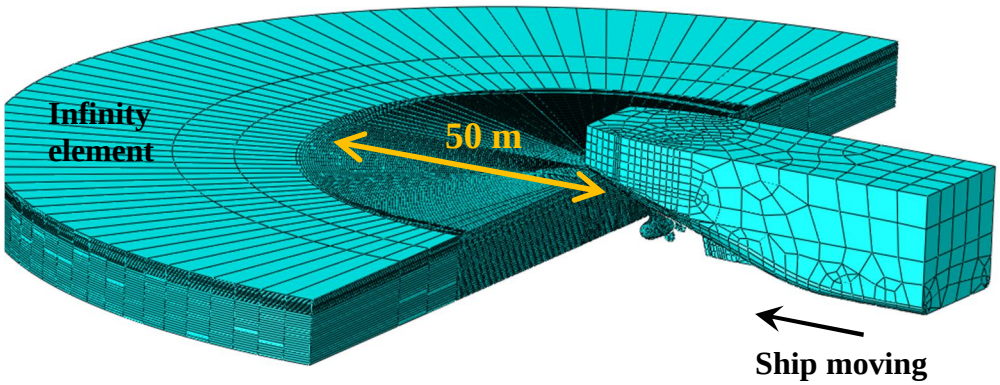

Figure 25. Extreme ridge + large hull.

6.2.2.5 Parametric run results

Table 5 and Table 6 introduce a summary of loads from the small thruster simulations and Table 7 and Table 8 correspondingly from the large thruster simulations. Simulation results (forces) are low-pass filtered with 10 Hz frequency.

Either the increase of ship velocity from two to four knots did not influence significantly on the ice loads or the results were inconsistent. Also, the variation of steering angle did not influence significantly. Typical ice ridge penetration loads were 3 - 8 MN for the small thruster and 8 – 15 MN for the large thruster. Figure 26 and Figure 27 introduce different ridge deformation types.

In vertical direction ice ridge push up hull and push down thrusters. Typical thruster vertical loads were 3 - 4 MN for the small thruster and 7 – 12 MN for the large thruster.

Table 5. Estimated small thruster ice ridge penetration loads on ship moving direction.

Ridge type	Thickness	Small thruster horizontal loads, MN					
		Speed 2 knot			Speed 4 knot		
		Angle 0°	Angle 45°	Angle 90°	Angle 0°	Angle 45°	Angle 90°
Typical	5.4 m	3.1	4.0	3.6	3.1	3.9	3.6
Extreme	10.8 m	6.0	-	6.0	6.3	8.1	8.1

Table 6. Estimated small thruster vertical loads (+ is downward).

Ridge type	Thickness	Small thruster vertical loads, MN					
		Speed 2 knot			Speed 4 knot		
		Angle 0°	Angle 45°	Angle 90°	Angle 0°	Angle 45°	Angle 90°
Typical	5.4 m	4.3	3.2	2.3	4.0	2.8	2.1
Extreme	10.8 m	4.3	-	3.0	4.5	3.9	3.5

Table 7. Estimated large thruster ice ridge penetration loads on ship moving direction.

Ridge type	Thickness	Large thruster horizontal loads, MN					
		Speed 2 knot			Speed 4 knot		
		Angle 0°	Angle 45°	Angle 90°	Angle 0°	Angle 45°	Angle 90°
Typical	5.4 m	6.8	8.0	8.5	6.7	9.8	7.0
Extreme	10.8 m	11.9	12.2	14.7	-	26.0	15.8

Table 8. Estimated large thruster vertical loads (+ is downward).

Ridge type	Thickness	Large thruster vertical loads, MN					
		Speed 2 knot			Speed 4 knot		
		Angle 0°	Angle 45°	Angle 90°	Angle 0°	Angle 45°	Angle 90°
Typical	5.4 m	7.1	8.2	6.5	8.6	7.5	5.8
Extreme	10.8 m	11.4	9.5	8.8	-	12.0	12.3

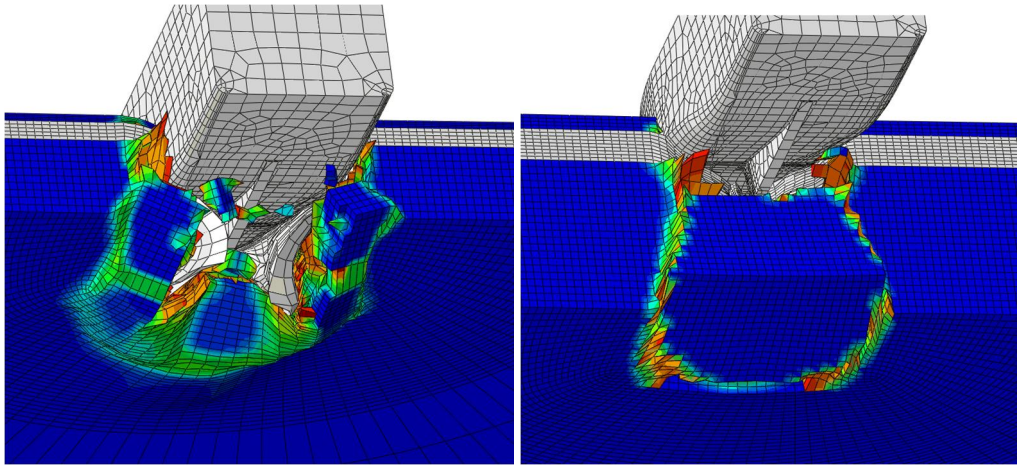

Figure 26. Ridge deformations with small ship. Left typical ridge and right extreme ridge.

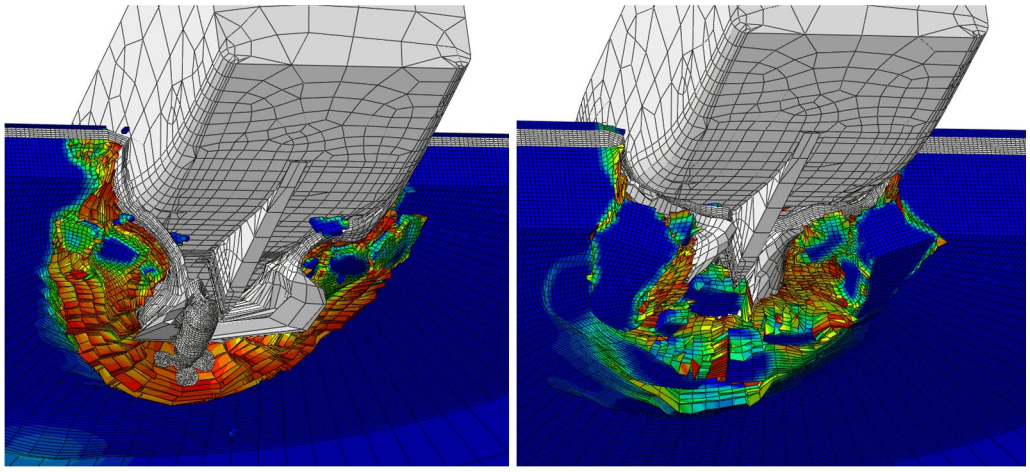

Figure 27. Ridge deformations with large ship. Left typical ridge and right extreme ridge.

6.2.3 Fennica case

6.2.3.1 Ice ridge

Total ridge height is 13.0 m (supposed constant) composed of 0.7 m rubble in the sail, 1.0 m consolidated layer and 11.3 m rubble in the keel. Figure 28 shows the dimensions of ridge.

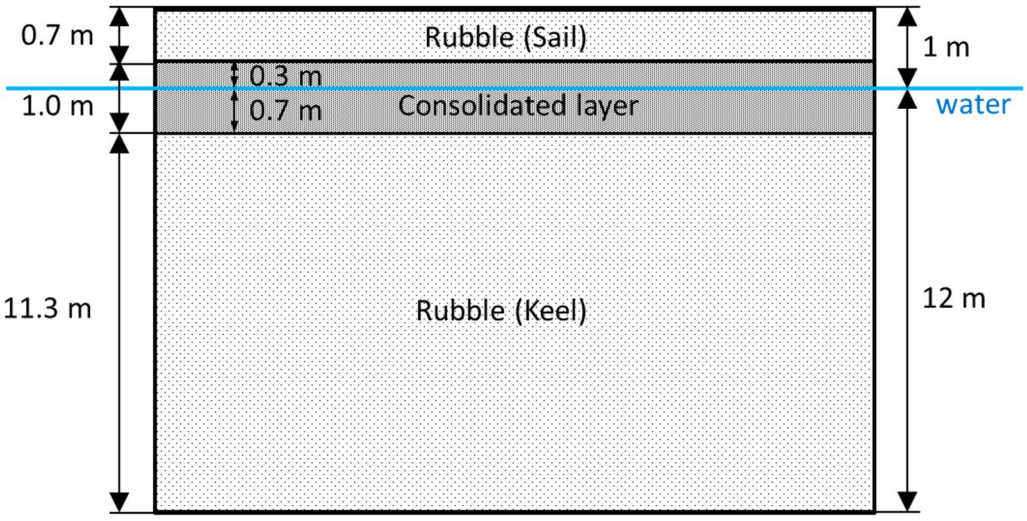

Figure 28. Ice ridge for Fennica case simulation.

6.2.3.2 Ice properties

Concrete Damaged Plasticity –model (CDP) was applied for the consolidated layer, as described in Ch. 6.2.2.2. The layer was divided into five layers in the thickness direction. The material properties of consolidated layer are introduced in Table 9.

Table 9. Consolidated layer ice properties.

Depth [m]	Temp. [°C]	E_{ave} [GPa]	E_{stdev} [GPa]	$S_{c,ave}$ [MPa]	$S_{c,stdev}$ [MPa]
0.1000	-2.0000	0.7047	0.3110	4.4022	1.6269
0.3000	-2.0000	0.9418	0.3300	6.2205	1.3964
0.5000	-2.0000	0.8441	0.2829	5.2418	0.9353
0.7000	-2.0000	0.5322	0.2036	3.3865	0.6634
0.9000	-2.0000	0.0881	0.0290	1.3789	0.4219

The material properties of ice rubble is describeded in Ch. 6.2.2.2.

6.2.3.3 Thrusters and hull

Thruster's total diameter is 5.3 m and propeller diameter 4.2 m. Number of blades is 4. Ship hull length is 116.0 m, width 26.0 m and draught 12.5 m. Thruster is shown in Figure 29 and hull in Figure 30.

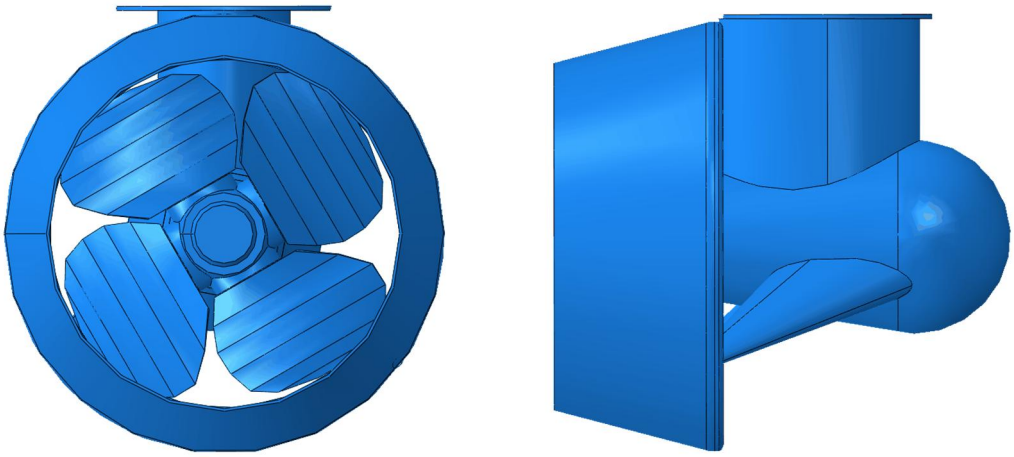

Figure 29. Fennica thruster model.

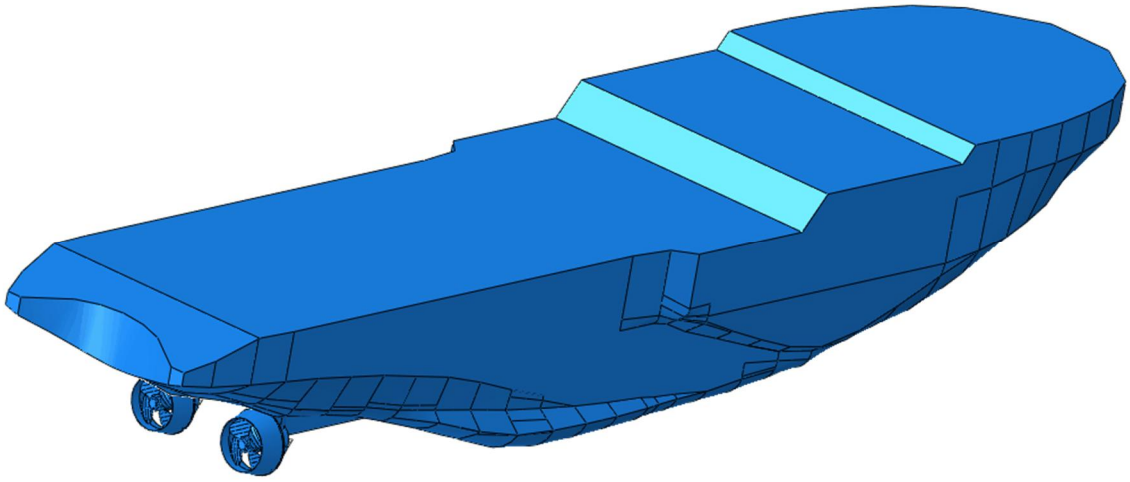

Figure 30. Fennica ship model.

6.2.3.4 FEM models and simulation

In middle part of the model was discretized with a dense element mesh (element size 400 – 500 mm), then sparse mesh (size 2.5 m) and infinity elements in the edge (40 m). In vertical direction the element size in the sail was 233 mm, in the consolidated layer 200 mm and in the rubble 404 mm. The model size was 100 x 200 m^2, dense mesh area 25 m and sparse mesh area 35 m. The number of elements in the model was 293945. Figure 31 introduces FEM-model.

Simulation variables were:

- ship initial speed is 5, 8 or 12 knot
- left thruster angle is -180° or -90°.

Numerical simulations were performed by Abaqus/explicit 6.12.1 program. Element types were C3D8R (ice), CIN3D8 (ice infinity), R3D3 and R3D4 (hull, thruster and propeller). The hull, thruster and propeller were assumed fully rigid. Simulation time was 10 s, corresponding 18-30 m movement of the ship

Simulation time was 10 s, in which the ship moved forward 18 – 30 m. Table 10 introduces used thruster angles.

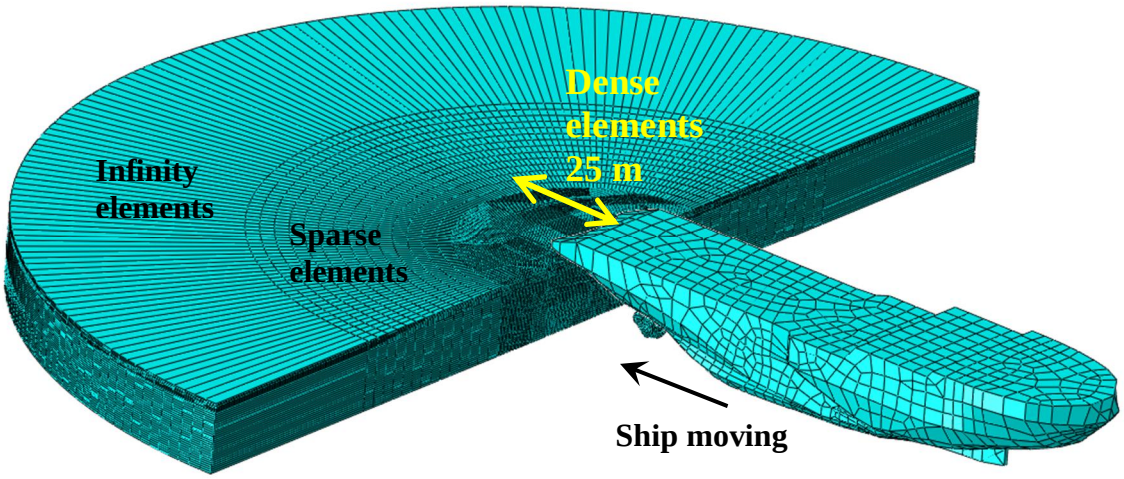

Figure 31. FEM model of Fennica in ridge penetration.

Table 10. Thruster angles in Fennica case simulation.

Angles	Left thruster	Right thruster
-180° / -180°	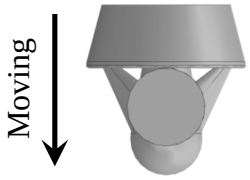	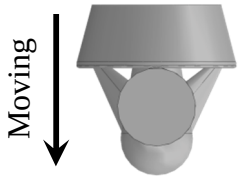

-90° / -180°	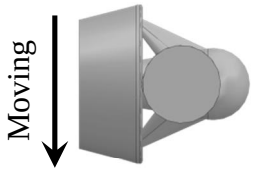	

6.2.3.5 Fennica case results

Table 11 introduces a summary of penetration loads from simulations.. Loads were printed at 0.05 s intervals and filtered by averaged 7 points. Figure 32 introduces simulated penetration loads as a function of ship speed. Respectively Figure 33 shows thruster load time history.

Increase of ship velocity from 5 to 8 knots or 8 to 12 knots increase ice loads about 1 MN. Turning of the left thruster (-90° steering angle) increase the penetration load 0.5 – 1.0 MN. Figure 34 to Figure 36 introduce different ridge deformation types and Figure 37 cutting of ridge after 12 knot simulations. Figure 38 shows effect of initial or constant ship speed. Decelerating ship speed causes clearly lower penetration loads.

Table 11. Estimated thruster loads during ice ridge penetration on ship moving direction.

Case	Thruster	Angle	Speed		
			5 knot	8 knot	12 knot
-180° / -180°	Left	-180°	1.6 MN	2.4 MN	3.5 MN
	Right	-180°	1.6 MN	2.4 MN	3.6 MN
-90° / -180°	Left	-90°	1.9 MN	2.9 MN	4.2 MN
	Right	-180°	1.5 MN	2.2 MN	3.3 MN

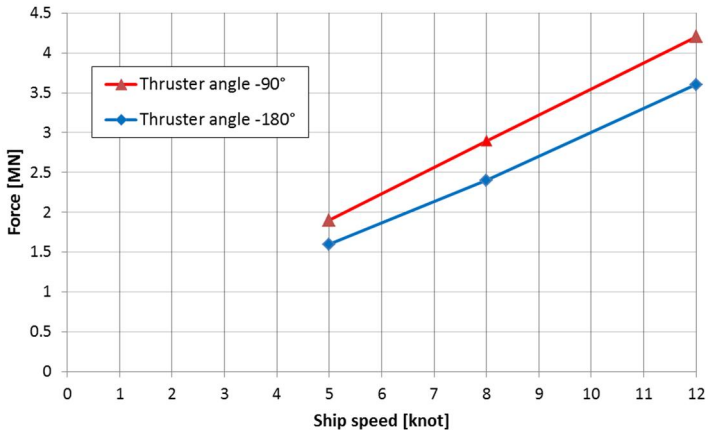

Figure 32. Simulated thruster penetration loads on ship moving direction by comparison ship speed.

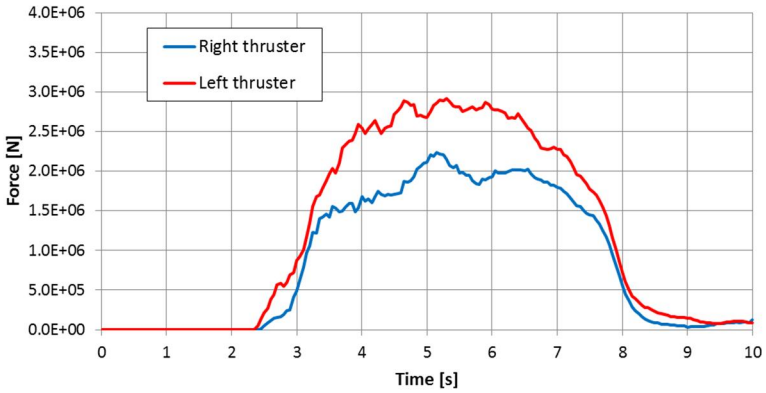

Figure 33. Simulated thruster penetration loads on ship moving direction by time. Red = PS thruster, angle 90 deg, blue = SB thruster, angle 180. Speed 8 knots.

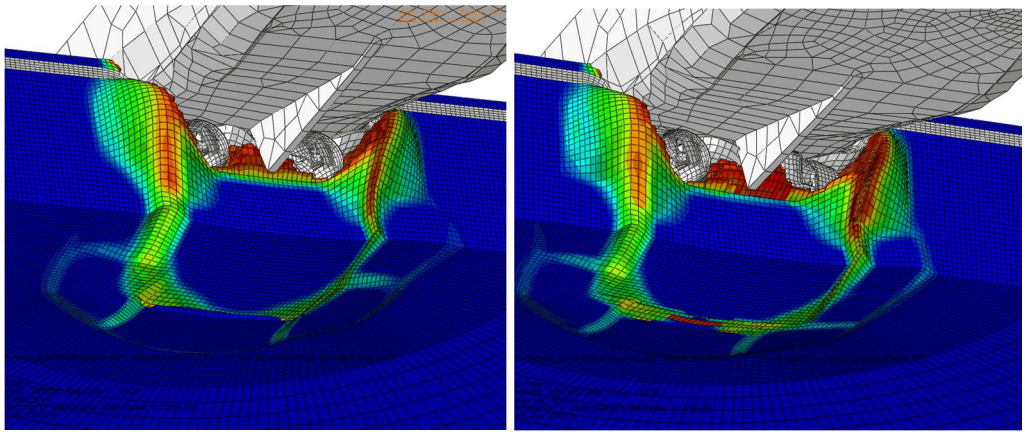

Figure 34. Ridge deformations after 5 knot simulations. Left: thruster angle -180° / -180°, right: thruster angle -90° / -180°.

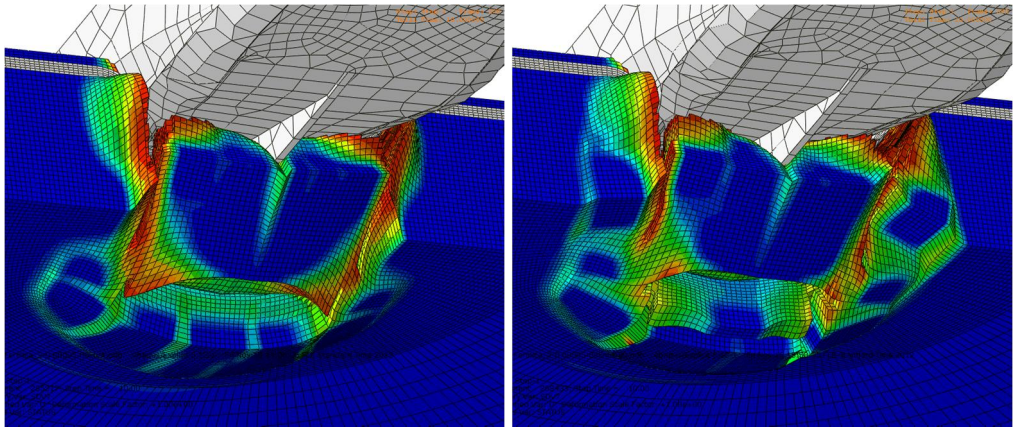

Figure 35. Ridge deformations after 8 knot simulations. Left: thruster angle -180° / -180°, right: thruster angle -90° / -180°.

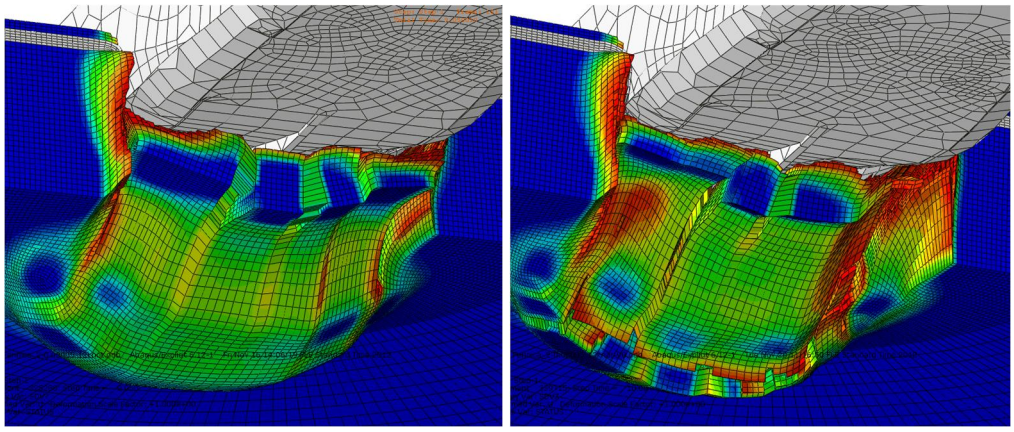

Figure 36. Ridge deformations after12 knot simulations. Left: thruster angle -180° / -180°, right: thruster angle -90° / -180°.

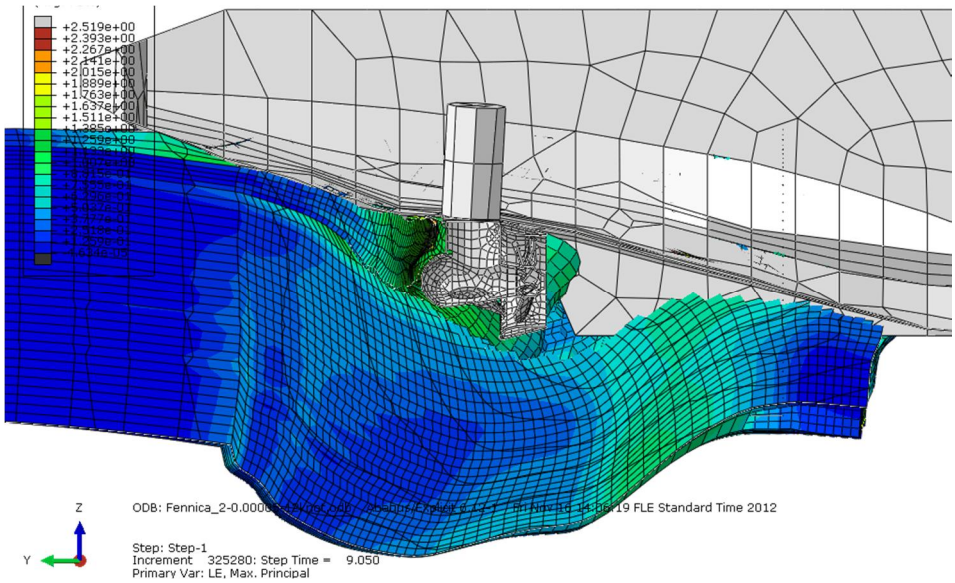

Figure 37. Cutting of ridge after 12 knot simulations. Thruster angles -180° / -180°.

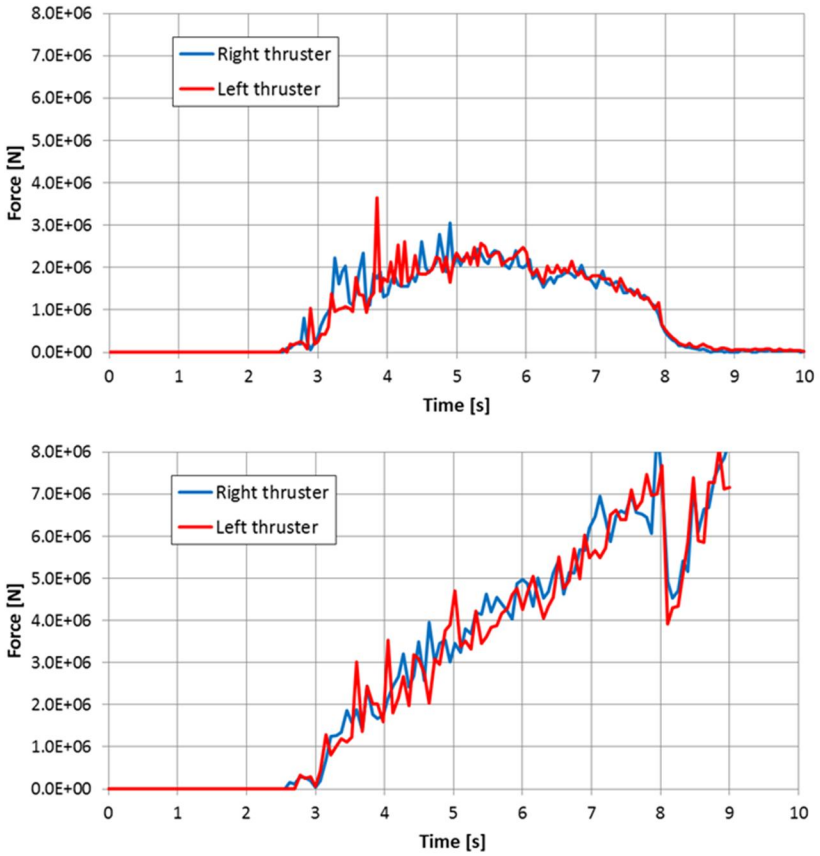

Figure 38. Comparison of initial and constant speed. Upper: initial speed, 8 knots. Lower: constant speed, 8 knots. Loads printed at 0.05 s intervals and not filtered.

6.2.4 Conclusions for ridge penetration

Summarizing the simulation parametric studies and the Fennica case, it is clear that significant difference between constant speed penetration and initial velocity penetration simulation was seen. The constant speed simulation gives high load values, whereas the initial velocity simulation seems most reasonable approach. Initial velocity simulation is recommended for load estimations.

Parametric case studies simulated during 2011 and 2012 likely gave too high loads because of constant speed ridge penetration.

Validation with Fennica full scale data shows somewhat higher simulated loads compared to measured loads. Qualitative behaviour of thruster loading is similar related to measurements when comparing thruster steering angles. Straight ahead penetration to ridge was simulated to give lower load than thruster turned sideways at same initial speed.

Simulation model does not include ship vertical motion and therefore simulated loads can be overestimated. This is a development point for further FEM simulation regarding ridge penetration.

Ice strength values for consolidated layer can be discussed, and may be too high.

Comparison of simulated and measured time histories show that timewise length of simulated load sequence correlates well with measured load sequence.

Also, simulation model gives load on thruster surface (pressure on surface), whereas measurement is total force response from structure. The measured signal is therefore mechanically filtered load signal.

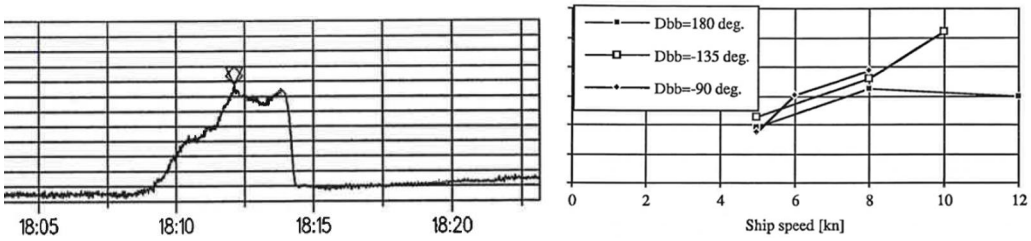

Figure 39. Fennica measured thruster loads. Left: longitudinal load by time, speed 8 kn, angle 91 deg. Right: Maximum loads by ship speed and angle.

6.2.5 Simplified effective pressure distribution

FEM simulations were utilized to introduce an effective pressure distribution on the thruster body. A simplified model was developed by introducing a number of layers with equal thicknesses. Each layer was attached with a constant pressure varying from layer to layer as shown in Figure 40. The pressure for each layer was selected as the highest value of the corresponding region during the time history analysis. Since the maximum values occurs at different times for each spot, this assumption results in a conservative ice load prediction. Therefore, further studies are needed to define more accurate estimate for the equivalent ice pressure distribution and corresponding resultant ice load.

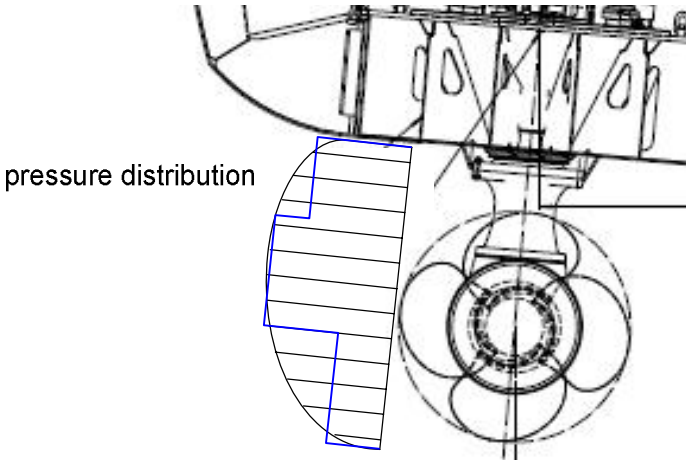

Figure 40. Theoretical load distribution from ridge interaction shown by black curvilinear line. Corresponding stepwise linear distribution is shown by blue line.

From the pressure distributions one can define the ice force (F_i) corresponding to each layer of thruster body and total force (F_{max}) as

$$F_i = p_i A_i \quad (20)$$

$$F_{max} = \sum_i F_i \quad (21)$$

in which p_i is the effective pressure for each layer and A_i is the corresponding projection area of the thruster.

7 Discussion

Modeling ice impact to structure originates to considering ice block kinetic energy at some initial impact speed and estimating contact load based on ice strength and contact surface properties. The structure dynamics are included in the model and during 2011-2012 work, ways to estimate structure damping effects, ice material elasticity effects, hydrodynamic nature of contact load between ice and structure and water flow induced drag force on impacting ice block were included in the model.

The impact model was applied to Fennica case and results compared with Fennica measurement data. Apparently, calculated impact contact loads may well be in correct range. However, the structure response measurement shows qualitatively different behaviour than the model estimates for structural response. In measurement, structure vibration response is significantly lower than model estimates. Further development and validation against measured data is needed. Creating laboratory test setup is also viable option.

For simulations of ship backing into ice ridge, years 2011 – 2012 have included a parametric study for effect of speed, thruster steering angle, thruster and ship size and ice ridge size. These were followed by modelling ice breaker Fennica hull and thrusters for actual case simulations.

Fennica case simulations were successfully run, and qualitatively, similar load behaviour to full scale measurement was observed in simulations. Simulated load levels were little higher than measured. Important finding from ridge penetration simulation was that using model with ship initial velocity gave rather realistic load behaviour, whereas ridge penetration with constant speed gives high load values. It is recommended to use the initial speed in ridge penetration modelling.

8 Conclusions

The project started in 2010, and the relevant load scenarios were chosen for closer inspection during that year. Continuation on 2011 included review of suitable load calculation methodology and first applications for load calculation. Also, right to use full scale data from measurements of Fennica and Botnica for validation within this project was obtained from the involved parties. The year 2012 has been further development of load calculation and applied methods.

It can be concluded that the impact load model give loads that are at a correct range but validation regarding the dynamic system excitation is still needed before the simplified load models can be formulated.

The ridge penetration model development show a good correlation with the full scale measurements and next step will be development of the simplified load model for ice class rules.

It has become evident that load models for the dynamic excitation for dynamic analysis are needed for the ice class rules. The proposal is to derive the load excitation based on the propeller ice load models that have been used for the development of the present Finnish Swedish Ice Class Rules for Propulsion Machinery.

References

Bjerkås, M. 2007. Review of measured full scale ice loads to fixed structures. Proceedings of the 26th International Conference on Offshore Mechanics and Arctic Engineering
(OMAE2007). San Diego, California, USA June 10-15, 2007, OMAE2007-29048

E. Richard Booser, CRC Handbook of Lubrication (Theory and Practice of Tribology) Volume II, CRC Press, 1983

Daley, C. 1999. Energy based ice collision forces. Expanded version of Proceedings of the 15th International Conference on Port and Ocean Engineering under Arctic Conditions (POAC 99). Espoo, Finland August 23-27, 1999.

Daley, C. and Yu, H. 2009. Assessment of ice loads on stern regions of ice class ships. International Conference on ship and Offshore Technology. Busan, Korea September 28-29, 2009.

DnV. 2010. Ice Strengthening of propulsion machinery. Classification Notes No. 51.1

Heinonen, J. (2004), Constitutive Modeling of Ice Rubble in First-Year Ridge Keel. VTT Publications 536, Espoo, 142 p., Doctoral Thesis, ISBN 951-38-6390-5 (URL:http://www.inf.vtt.fi/pdf/)

Huovinen, S. 1990. Abrasion of concrete by ice in arctic sea structures 1990 VTT Publication nr 62 Espoo 110 p. app 31 p. Test arrangement P.93

http://ahravuo.vtt.fi/
AHRAVUO - Ridge-structure interaction simulation, Project www-pages

VTT Ship Laboratory. Research report No. LAI-2663/93. Espoo, 11.10.1993.